

Transoesophageal echocardiography in adult congenital heart disease

N D Masani

Department of
Cardiology, University
Hospital of Wales,
Heath Park, Cardiff
CF14 4XW
N D Masani

Correspondence to:
Dr Masani
navroz.masani@
cardiffandvale.wales.nhs.uk

The diagnosis of congenital heart disease de novo in adults is now uncommon. Increasing numbers of children with congenital heart disease are surviving to adulthood, leading to the development of adult congenital heart disease as a distinct subspecialty.¹ Nevertheless, adults with congenital heart disease still present to general cardiologists—as an initial presentation, for geographical or logistic reasons, during acute or concurrent illness, or through loss of regular follow up. Echocardiography is the mainstay of diagnostic imaging in adult congenital heart disease—its role in the spectrum of congenital heart disease most often encountered in adults has been reviewed comprehensively.² However, precordial windows in these patients are often suboptimal because of previous surgery, chest deformity or lung disease. Multiplane transoesophageal echocardiography (TOE) has proven to be of great value in adult congenital heart disease because of its high resolution, clear acoustic windows, proximity to posterior cardiac structures, and comprehensive imaging planes.³

In the diagnosis of congenital heart disease, the echocardiographic examination is performed in a detailed, systematic manner. This requires a protocol and mindset that differs from the approach often used in TOE in the adult cardiology setting. The purpose of this

paper is to describe an approach to TOE in adult congenital heart disease. Specific emphasis is placed on those conditions that present in adulthood and that involve detailed TOE views of structures rarely necessary in general cardiology. The echocardiographic approach to patients who have undergone palliative procedures (for example, Mustard or Senning repairs, Fontan operations) are touched upon briefly; the echocardiographic approach to them has been discussed previously.² The use of TOE during interventional and surgical procedures is beyond the remit of this paper.

General considerations

Clinical training and experience in congenital heart disease, as well as expertise in echocardiography, are invaluable. The former to recognise the morphologic patterns, variations, clinical associations, and complications of adult congenital heart disease, the latter to appreciate the complex echo-anatomic relations that may be encountered. The advice of a cardiologist specialising in congenital heart disease (paediatric or adult), to complement the skills of the TOE operator during the study, is helpful in complex cases. TOE should be regarded as part of an integrated imaging approach combined with other complementary techniques, in particular transthoracic echocardiography, cardiac magnetic resonance imaging, and angiography.⁴ Detailed patient information should be sought; however, diagnoses made in childhood should not be assumed to be complete.

TOE protocol for adult congenital heart disease

For all cases, it is important to develop and follow a structured comprehensive protocol, utilising multiplane views and all of the available windows (upper and mid oesophageal, gastro-oesophageal junction, mid gastric, and deep gastric). We use a systematic approach adapted from that used in adult patients with acquired cardiac disease (table 1). It is important to understand the segmental approach to scanning in congenital heart disease.⁵ Although this is best suited to transthoracic echocardiography (TTE), the TOE study should also start by establishing (or confirming) cardiac situs and connections, as outlined in table 2. The high resolution of TOE confers an advantage over TTE in the identification of the defining characteristics of cardiac structures (table 3), particularly the atrial appendages.

Table 1 A protocol for transoesophageal echocardiography in adult congenital heart disease

1. Establish cardiac situs and connections as defined in table 3
2. Examine the morphology and function (two dimensional echo), flow and haemodynamics (colour and spectral Doppler) of each structure as follows:

Protocol	Assessment	Examples
Systemic "circuit"		
Atrium	Atrial morphology Pulmonary venous connections Pulmonary venous baffle Atrial septum	Cor triatriatum Anomalous drainage Mustard/Senning ASD
AV connection	Atrioventricular septum AV valve morphology	Partial, intermediate, complete AVSD Cleft, accessory, parachute mitral valve Supramitral ring
Ventricle	Morphology, size and function Ventricular septum Outflow tract	VSD Subaortic membrane, tunnel, HOCM Bicuspid, etc.
VA connection	Aortic valve	Transposition, Malposition etc.
Great artery	Aorta	Truncus arteriosus PDA, aortopulmonary window Coarctation Blalock-Taussig, Waterston, Potts shunts
Pulmonary "circuit"		
Atrium	Atrial morphology Coronary sinus	Fontan connections Left SVC, unroofed CS Ebsteins anomaly
AV connection	AV valve morphology	
Ventricle	Morphology, size and function Outflow tract	Right ventricular infundibular stenosis Double chamber right ventricle Tetralogy of Fallot
VA connection	Pulmonary valve	Bicuspid, etc.
Great artery	Pulmonary arteries	Supra PS Branch PS

AV, atrioventricular; ASD, atrial septal defect; AVSD, atrioventricular septal defect; CS, coronary sinus; HOCM, hypertrophic obstructive cardiomyopathy; PDA, patent ductus arteriosus; PS, pulmonary stenosis; SVC, superior vena cava; VA, ventriculoatrial; VSD, ventricular septal defect.

Table 2 The segmental approach to congenital heart disease

Segment	
Atria	Atrial situs Atrial morphology Veno-atrial connections
Atrioventricular connection	Concordant or discordant AV valve morphology
Ventricles	Ventricular morphology
Ventriculo-arterial connection	Concordant or discordant Outflow tract morphology VA valve morphology Great arteries

AV, atrioventricular; VA, ventriculoatrial.

Table 3 Defining characteristics of the cardiac chambers

Structure	Characteristic appearance
Right atrium	Systemic venous connections Wide necked, blunt appendage
Left atrium	Narrow necked, hook like appendage
Right ventricle	Tricuspid valve offset apically Chordal attachments to the ventricular septum Triangular shape with separate inflow/body/outflow Moderator band Trabeculated endocardial surface
Left ventricle	Mitral valve offset basally Two papillary muscles—no chordal insertion to septum Ellipsoid shape with adjacent inflow and outflow tracts



Figure 1 The atrial septum is seen in a vertical plane (90°), from the superior vena cava/right atrium junction to the inferior vena cava/right atrium junction. Right atrial morphology is well appreciated in this “bicaval view”, including the broad, wide necked appendage (arrow). In this patient, the right atrium is dilated and there is a defect in the fossa ovalis region of the atrial septum (secundum atrial septal defect). IVC, inferior vena cava; SVC, superior vena cava; RA, right atrium; LA, left atrium.

ASSESSMENT OF THE RIGHT ATRIUM AND SYSTEMIC VEINS

Differentiation of the right atrium (RA) from the left atrium (LA) is based on identification of the appendages—the characteristic broad mouthed, blunt appearance of the RA appendage is best appreciated in the vertical plane (90°)—the “bicaval view” (fig 1). The christa terminalis may be seen as a linear structure seen extending from the RA wall close to the inferior vena cava (IVC) to the septum adjacent to the superior vena cava (SVC). This can be mistaken for the atrial septum, leading to a false diagnosis of atrial septal defect (ASD). Agitated saline contrast (injected into the left arm, see below) is used to identify the systemic venous connections to their respective atrium and detect intracardiac right-to-left shunts.



Figure 2 The relation between the superior vena cava (seen in short axis, superior to its junction with the right atrium) and the right sided pulmonary veins is seen from an upper oesophageal view, at 0° (A). The right upper pulmonary vein enters the left atrium “vertically”, while the origin of the right lower pulmonary vein is seen in a horizontal orientation (arrow). In the same view (B), a communication is seen between the right upper and lower pulmonary veins, superior vena cava and left atrium, in a patient with sinus venosus atrial septal defect and partial anomalous pulmonary venous drainage. In the same patient, an oblique view, similar to the bicaval view (C), shows the superior vena cava overriding the upper atrial septum (arrow) at which point the superior sinus venosus defect, with a left-to-right shunt, can be seen. RUPV, right upper pulmonary vein; RLPV, right lower pulmonary vein; SVC, superior vena cava; RA, right atrium; LA, left atrium; IVC, inferior vena cava.

The SVC is scanned in its transverse plane at 0° , from the upper oesophageal window (fig 2) down to the SVC/RA junction. This manoeuvre is used to identify anomalous pulmonary venous drainage (PAPVD) into the SVC/RA junction and superior sinus venosus ASD. By rotating the imaging plane to 90° the distal SVC is seen in its long axis (fig 1). The course of the IVC is difficult to visualise in adults. In the transgastric view at 0° , the IVC may be seen in cross section—rotation of the image plane until it appears in its long axis allows visualisation of its drainage into the RA. From the transoesophageal views, only its junction with the RA is seen (note the

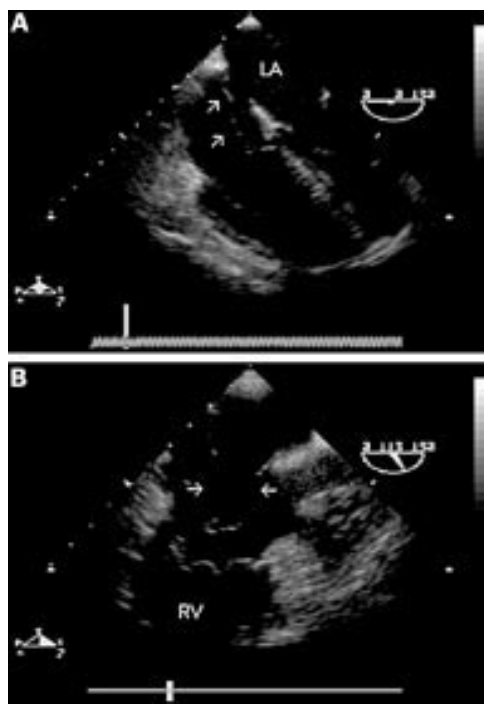


Figure 3 Mid oesophageal four chamber view (0°) (A) showing an atrial septal aneurysm and secundum defect. There is a mobile “wind sock” appearance of the mid portion of the atrial septum. A long axis view of the right heart (110°) (B) shows two large defects in the aneurysmal part of the septum (arrows). The entire defect was closed using a single percutaneous catheter based occlusion device. RV, right ventricle; LA, left atrium.

variable appearance of the eustachian valve at this site). This is best done by advancing the probe slightly in the biatrial view (90°).

The coronary sinus is seen in the horizontal plane (0°) by advancing the probe from the mid oesophageal window to the gastro-oesophageal junction, where it is seen traversing the atrio-ventricular groove behind the LA before entering the RA. A communication between the coronary sinus and the left atrium may occur (“unroofed coronary sinus”). For depicting the relation between the coronary sinus and an ASD, an oblique (130°) mid oesophageal view is useful. Pronounced dilatation of the coronary sinus, in the presence of normal RA pressure, is suggestive of persistent left SVC—diagnosed by following the course of the coronary sinus back to a vertically orientated

Table 4 Suitability of secundum atrial septal defect for transcatheter device closure

View	TOE measurements (mm)
Any	Largest dimension of defect (2DE) Largest dimension of defect (CFM)
Mid oesophageal four chamber view	Inferior rim of defect to MV Inferior rim of defect to TV Total septal length
Short axis view at base of heart	Antero-superior rim of defect (to aortic root) Posterior rim of defect (to pulmonary vein) Total septal length
G-O junction (0°) or oblique (130°) coronary sinus view	Inferior rim of defect to coronary sinus
Biatrial view	Superior rim of defect to SVC Inferior rim of defect to IVC Total septal length

2DE, two dimensional echocardiography; CFM, colour flow mapping; G-O, gastro-oesophageal; IVC, inferior vena cava; MV, mitral valve; SVC, superior vena cava; TV, tricuspid valve.

vein and/or observing the wash-in of contrast injected into a left upper limb vein.

ASSESSMENT OF THE LEFT ATRIUM AND PULMONARY VEINS

The narrow hook shaped LA appendage is best seen by flexion/withdrawal of the probe from the mid oesophageal (four chamber) position. The pulmonary veins are difficult to examine by TTE in the adult but can be well seen by TOE. All four pulmonary veins entering the LA should be seen during routine TOE examination. The orientation of the upper pulmonary veins is more vertical, while that of the lower pulmonary veins is more horizontal. The left upper pulmonary vein is identifiable running above and parallel to the appendage, with the typical venous flow pattern toward the LA. Alignment along its long axis may be improved by rotating the imaging plane up to approximately 60°. Slight advancement of the probe (at 0°) enables the origin of the left lower pulmonary vein to be seen. At the same level in the oesophagus, rotation of the probe to the right brings the right lower pulmonary vein into view (fig 2). Slight withdrawal of the probe reveals the right upper pulmonary vein. The probe should be withdrawn to interrogate the relation between the right upper pulmonary vein and SVC.

ABNORMALITIES OF THE ATRIA AND VENOUS DRAINAGE

Cor triatriatum

Although this is a very rare condition, it may present in adulthood. It is characterised by a membrane in the left atrium, obstructing pulmonary venous return within the LA cavity. The appearance of a membrane within the left atrium associated with obstructive flow patterns on colour flow mapping and spectral Doppler gradients are typical.

Partial anomalous pulmonary venous drainage (PAPVD)

This often accompanies sinus venosus ASD. Most commonly, the right upper and/or right lower pulmonary vein(s) drain into the SVC or SVC/RA junction (fig 2). More complex forms of PAPVD (including supra and infracardiac types) are rarely seen de novo in adults and are better diagnosed by magnetic resonance imaging.

Surgically corrected partial or total anomalous pulmonary venous drainage may require reinvestigation to determine the patency of the venous connection. Visualisation of the distorted vessels may be difficult, exacerbated by the echodensity of surgical patch/baffle material. The presence of turbulence on colour flow mapping should be noted, and spectral Doppler is mandatory (an example of an obstructed pulmonary venous connection is seen in fig 11).

ASSESSMENT OF THE ATRIAL SEPTUM AND ATRIAL SEPTAL DEFECT

It is important to interrogate the entire atrial septum to ensure that small defects at the margins of the septum are not missed. In the horizontal plane (0°) the entire septum is

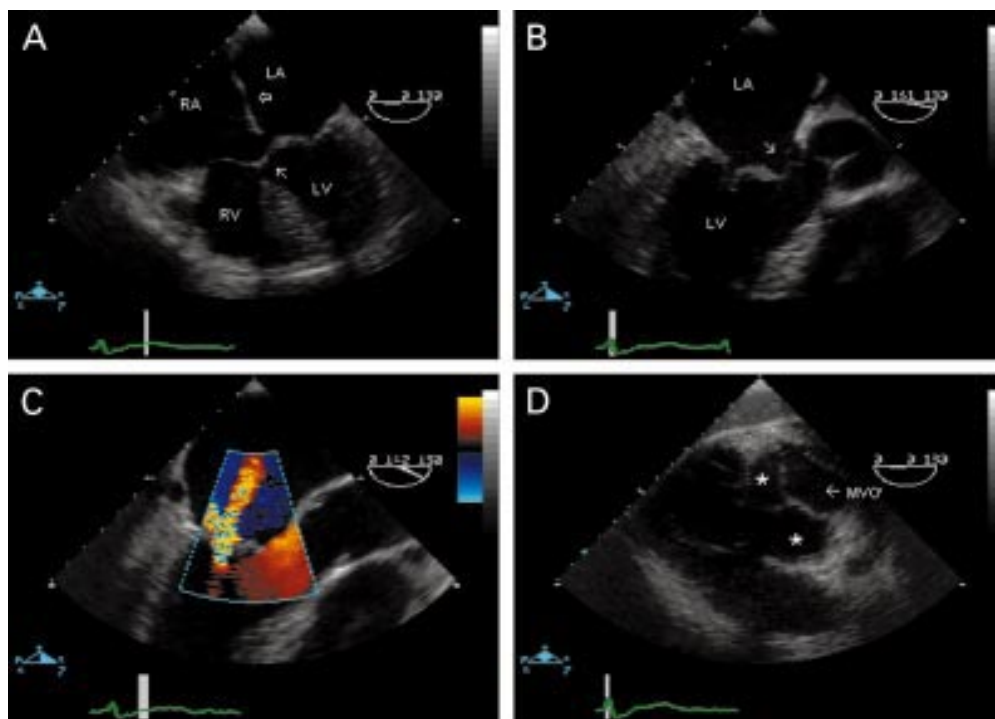


Figure 4 Partial atrioventricular septal defect seen in a four chamber view (A). There is a primum atrial septal defect (unmarked) and also a small secundum defect (open arrow). There is loss of offsetting of the atrioventricular valves, which insert into the crest of the ventricular septum giving the appearance of thinning at this point (closed arrow). In an oblique, long axis view of the left ventricle (B), deformity of the anterior leaflet of the left atrioventricular (“mitral”) valve is seen (arrow). Colour flow mapping in the same view (C) reveals valvar regurgitation through the commissural orifice, not through the apparent “cleft”, which is intact. From the transgastric position (D), deep flexion of the probe produces images of the atrioventricular valves in cross section. The “mitral valve” orifice is marked (MVO). The anterior leaflet can be seen divided by a “cleft” into superior and inferior components (*). LA, left atrium; LV, left ventricle; MVO, left atrioventricular valve orifice.

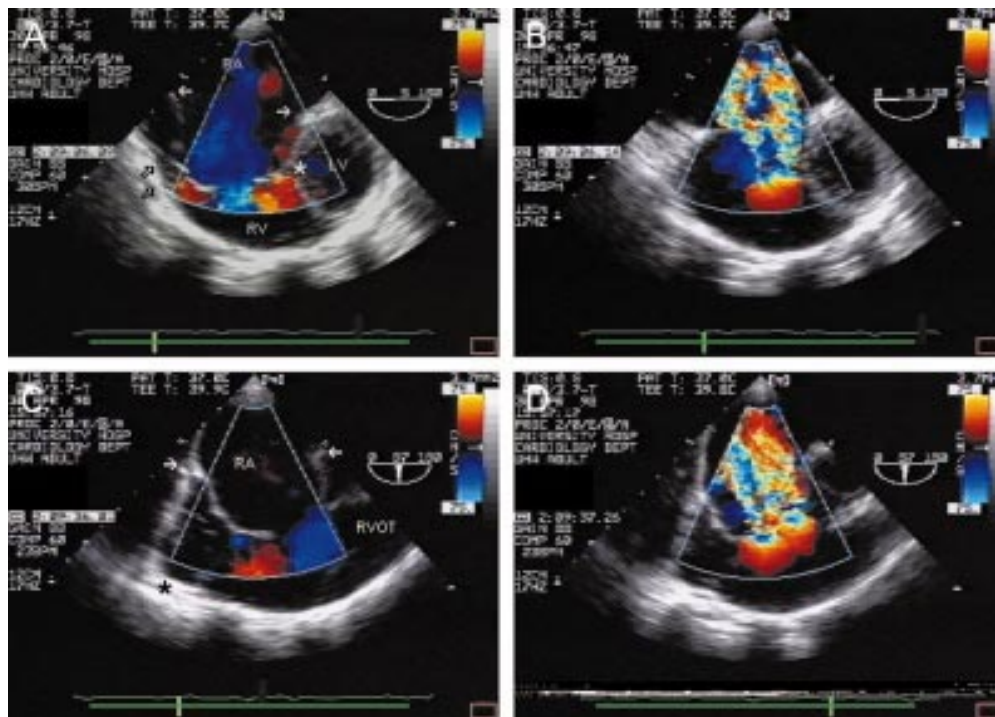


Figure 5 Ebstein’s anomaly. From a modified four chamber view at the gastro-oesophageal junction (A), the right atrium is seen to be severely dilated. The closed arrows indicate the level of the tricuspid annulus. There is atrialisation of a large part of the right ventricular cavity. The septal leaflet is displaced downward from the annulus (*) and the anterosuperior tricuspid valve leaflet is large and abnormally tethered to the right ventricular wall (open arrows). In B, colour flow mapping reveals very severe tricuspid regurgitation, through a regurgitant orifice well below the tricuspid valve annulus. Oblique views of the right sided structures are often helpful; C shows multiple abnormal “chordae” tethering the large anterosuperior leaflet to the right ventricular wall (*). In systole (D), severe tricuspid regurgitation is seen through two regurgitant orifices (that is, two flow convergence zones). RA, right atrium; RV, right ventricle; LV, left ventricle; RVOT, right ventricular outflow tract.

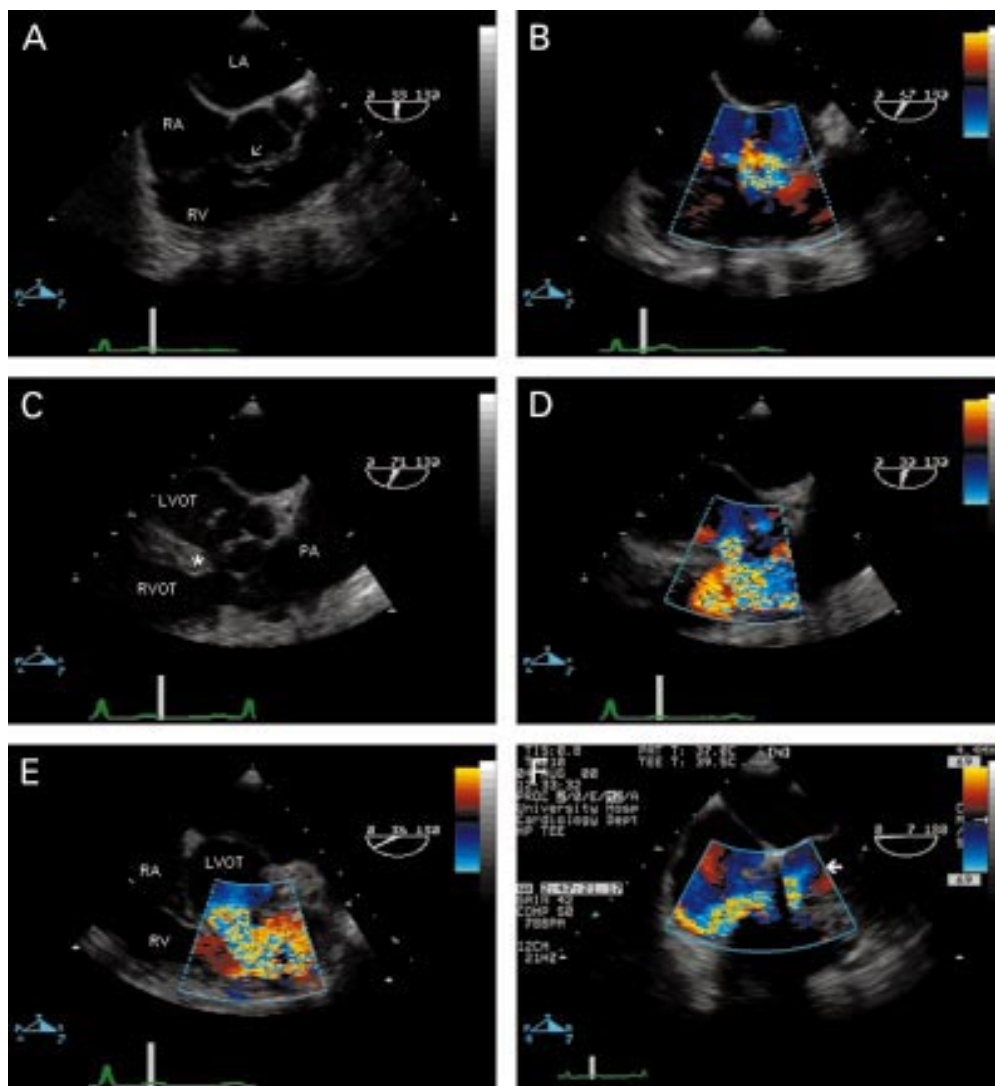


Figure 6 Ventricular septal defect (VSD) seen in the transverse plane of the left ventricular outflow tract (A). There is a defect in the perimembraneous region (arrow), partially plugged by tricuspid valve tissue. Colour flow mapping (B) reveals the presence of a left-to-right shunt—note the flow convergence zone in the left ventricular outflow tract—confirming the diagnosis of perimembraneous VSD. (C) Oblique view showing the right ventricular outflow tract in its long axis, in a patient with aortic valve endocarditis—note the vegetation seen in the left ventricular outflow tract. There is a defect seen between the two outflow tracts (*). The right ventricular infundibulum is hypertrophied, resulting in the appearance of subpulmonary stenosis, and the pulmonary artery is dilated. The diagnosis of doubly committed VSD is confirmed by colour flow mapping (D). (E) The same defect in the short axis view. Note that the defect is between left ventricular outflow tract and right ventricular outlet rather than between left ventricular outflow tract and right ventricular inlet as with perimembraneous defects (B). The importance of the flow convergence zone is demonstrated in F. The four chamber view with flexion reveals the left ventricular outflow tract in a patient with two previous aortic valve replacements. An apparent jet of tricuspid regurgitation is seen in the right atrium. However, note that this flow originates from the left ventricular outflow tract (arrow)—that is, there is a communication between the left and right ventricle. The dropout within the colour map is caused by artefact from the aortic valve replacement. RA, right atrium; RV, right ventricle; LV, left ventricle; RVOT, right ventricular outflow tract; LVOT, left ventricular outflow tract; LA, left atrium; PA, pulmonary artery.

interrogated, from the SVC/RA superiorly to the coronary sinus/RA junction inferiorly. Rotation of the image plane to the bicaval view (90°) displays the septum in an orthogonal plane, from IVC to SVC, thereby ensuring that inferior and superior sinus venosus ASDs (fig 2) are not missed.

Ostium secundum ASD

The secundum septum may be mobile, aneurysmal, contain a patent foramen ovale or septal defect—the most common de novo adult congenital heart disease diagnosis (fig 3). The presence of an ASD is confirmed by the use of colour flow mapping. Care should be taken not to misdiagnose colour flow mapping jets

entering the RA from the vena cavae or coronary sinus. TOE is valuable in confirming the diagnosis, identifying associated defects, and assessing suitability of the defect for percutaneous device closure (table 4).

Sinus venosus ASD

The superior form of this defect is more commonly encountered, often associated with PAPVD. The SVC overrides the atrial septum, seen best in the biatrial view (90°) (fig 2).

Ostium primum ASD, partial and intermediate atrioventricular septal defect (AVSD)

This defect may include abnormal development of the atrioventricular (AV) septal region and

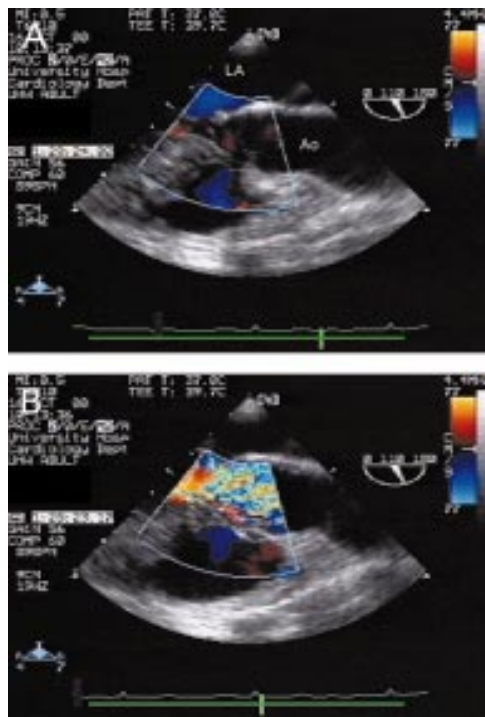


Figure 7 Long axis view of the left ventricular outflow tract (within the colour flow mapping box) and aortic root (A). A membrane is seen attached to the anterior mitral valve leaflet and the ventricular septum causing severe narrowing of the left ventricular outflow tract approximately 1 cm below the aortic valve. There is pronounced left ventricular hypertrophy. Colour flow mapping (B) in the same view reveals turbulence and a flow convergence zone proximal to the aortic valve. LA, left atrium; Ao, aorta.

valves, all of which must be assessed in detail. Partial AVSD (ostium primum ASD) affects the inferior part of the atrial septum and the AV valves; it may present in adulthood. The left AV valve usually has three leaflets (the anterior leaflet divided into superior and inferior parts by a “cleft”). Both AV leaflets insert into the crest of the ventricular septum, thereby “sealing off” an interventricular connection, often giving the upper septum an aneurysmal appearance (fig 4).

These defects are readily visualised in the mid oesophageal views. The value of TOE lies in detailing the morphology of the left AV valve and identifying associated defects. The cleft in the “anterior” leaflet may appear as a fold (fig 4) or cleft between the superior and inferior leaflets. Regurgitation may occur through the “cleft” as well as the normal leaflet orifice and this is identified by colour flow mapping. This is best seen at 0°, flexing slightly to interrogate the superior part of the anterior leaflet and by scanning through the valve from 0° to 130° where it is seen lengthways (fig 4). The chordal arrangement of both AV valves should also be assessed and can be performed by scanning up and down the transverse plane. Short axis transgastric views of the AV valves are obtained by careful full flexion of the probe at 0°. This may show the position of each leaflet (fig 4) and the site of regurgitation.

Complete AVSD, comprising an additional inlet ventricular septal defect and a common AV valve with five leaflets, is rarely encountered in adults. However, intermediate forms occur,

with only partial closure of the ventricular septum by the atrioventricular valve attachments. A separate interrogation of this region is required—in common with other unusual or variable findings, this can be done efficiently by keeping the region of interest in the centre of the scan sector and performing a careful 180° sweep, first with two dimensional echo and then colour flow mapping.

Repaired AVSD

Repair of the left AV valve in childhood may restrict leaflet mobility, leading to stenosis and/or regurgitation through the cleft or the normal orifice. Left ventricular outflow tract obstruction may also be a late feature.

ATRIOVENTRICULAR VALVES

Congenital defects of the AV valves rarely present in adulthood. Only Ebstein’s anomaly is considered here.

Ebstein’s anomaly

This condition covers a spectrum of disease in which there is apical displacement of the origin (hinge point) of one or more tricuspid valve leaflet, from the AV junction into the RV cavity. The septal leaflet is most commonly affected. The anterosuperior leaflet may not be displaced but is commonly abnormally large, with anomalous attachments to the RV wall and apex. The tricuspid valve leaflets are often dysplastic. The “atrialisation” of the RV, together with a variable degree of RV wall dysplasia, severe tricuspid regurgitation, and occasionally tricuspid stenosis, result in a small, restrictive RV. There is often an ASD and, depending on the RA pressure and degree of tricuspid regurgitation, shunt flow may be right-to-left.

The diagnosis is usually made in the four chamber view (often better by TTE than TOE) (fig 5). The image plane is rotated to the short axis view (30–50°) and further until a long axis image of the RA, tricuspid valve, and RV is obtained (the angle at which this plane is obtained is variable) in which the abnormal morphology and distal attachments of the anterosuperior leaflet can be seen. In view of the variable morphology of these valves and the frequent association with severe dilatation of the right atrium, it is helpful to complete a full 180° sweep of the tricuspid valve, first with two dimensional echo, then colour flow mapping. It is very important, in the surgical workup of these patients, to determine the presence of tricuspid stenosis and the severity, site and mechanism of tricuspid regurgitation. In the adult patient this may be caused by the defect itself, superimposed damage due to endocarditis, leaflet rupture or perforation. These details are useful in predicting those patients in whom repair of the tricuspid valve may be possible (in particular the degree of leaflet tethering and “atrialisation of the RV”).

Congenitally corrected transposition of the great arteries (TGA)

It is important to recognise this rare condition, in which there is atrioventricular and ventriculo-arterial discordance resulting in a



Figure 8 Short axis view at the aortic valve leaflet tips showing many characteristics of congenital bicuspid aortic valve: there is fusion of the left (L) and right (R) cusps. The raphe gives the appearance of a commissure dividing the valve into three leaflets when closed. The valve orifice during systole is oval shaped rather than triangular. The sinuses are asymmetric and unequal in size. The aortic valve area can be measured accurately by planimetry in this view. R, right coronary cusp; L, left coronary cusp; N, non-coronary cusp.

circulation that may function normally well into adulthood. The echocardiographic features are those of RV morphology in the systemic ventricular position and left ventricular (LV) morphology in the subpulmonary

ventricular position. A common feature of conditions in which there is malposition of the great arteries is a parallel arrangement rather than the normal arrangement in which they are perpendicular to each other (see fig 11F). There may be associated tricuspid regurgitation (either from dysplasia of the valve or annular dilatation). In complex forms of the condition, there may be coexistent ventricular septal defect (VSD) and pulmonary stenosis.

ASSESSMENT OF THE VENTRICULAR SEPTUM AND VENTRICULAR SEPTAL DEFECT

The ventricular septum is a complex structure that requires careful interrogation in multiple planes. From the mid oesophageal window (0°), flexion displays the left ventricular outflow tract (LVOT) and thin membranous part of the septum (see perimembranous VSD). Advancing the probe reveals the muscular/trabecular part of the septum (see muscular VSD) but it may be impossible to fully interrogate the apex in this view. Image plane rotation to 30–45° produces a short axis view of the heart analogous to an inverted parasternal short axis view. By rotating the probe to image in a plane passing below the level of

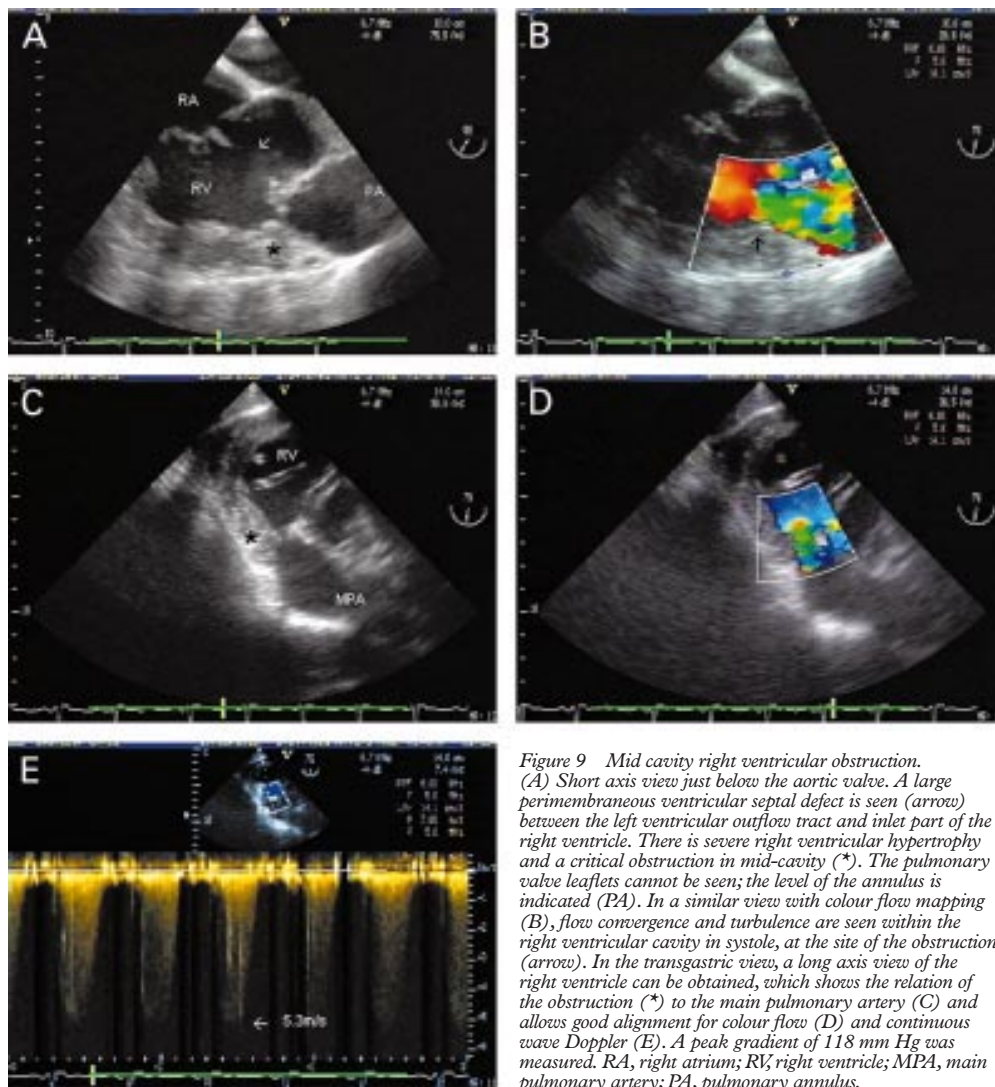


Figure 9 Mid cavity right ventricular obstruction. (A) Short axis view just below the aortic valve. A large perimembranous ventricular septal defect is seen (arrow) between the left ventricular outflow tract and inlet part of the right ventricle. There is severe right ventricular hypertrophy and a critical obstruction in mid-cavity (*). The pulmonary valve leaflets cannot be seen; the level of the annulus is indicated (PA). In a similar view with colour flow mapping (B), flow convergence and turbulence are seen within the right ventricular cavity in systole, at the site of the obstruction (arrow). In the transgastric view, a long axis view of the right ventricle can be obtained, which shows the relation of the obstruction (*) to the main pulmonary artery (C) and allows good alignment for colour flow (D) and continuous wave Doppler (E). A peak gradient of 118 mm Hg was measured. RA, right atrium; RV, right ventricle; MPA, main pulmonary artery; PA, pulmonary annulus.



Figure 10 Pulmonary stenosis in a patient who had been misdiagnosed as having a ventricular septal defect 30 years earlier. The short axis view (A) shows the triangular orifice of a tricuspid aortic valve (see fig 8). Doming of the pulmonary leaflets (arrows) is seen in A and B. This relatively subtle feature is easy to miss but was indicative of severe pulmonary stenosis in this case. There is “post-stenotic” dilatation of the main pulmonary artery. The right ventricular wall is hypertrophied but the infundibulum is not narrowed. The transgastric view (C) allows good alignment of the Doppler signal with flow. A peak gradient of 84 mm Hg was obtained in this case. RA, right atrium; RV, right ventricle.

the aortic valve, perimembraneous and doubly committed VSD can be seen and differentiated (fig 6). Further rotation of the image plane to 130° produces an approximation of the apical long axis view (fig 6) providing further imaging of the perimembraneous septum, another imaging plane through the muscular septum, and an ideal view to identify an overriding septum (that is, tetralogy of Fallot). Having performed the two dimensional echo sweep, this is repeated using colour flow mapping. Although it may be difficult to align the Doppler beam parallel to VSD flow, it is important to look out for turbulence within the RV cavity and a flow convergence zone within the LV cavity (fig 6). In order to interrogate the muscular septum fully, a transgastric transverse (0°) image is obtained and swept from its highest point to its

deepest, first by two dimensional echo. From the deep fundal view, a view analogous to the apical TTE views may be obtained and this provides excellent imaging of the apex.

In patients with perimembraneous VSD, TOE is valuable in identifying the mechanism of spontaneous closure and associated findings—for example, suction of the right aortic cusp into the defect resulting in aortic regurgitation or involvement of tricuspid subvalvar tissue.

ASSESSMENT OF LEFT VENTRICULAR OUTFLOW AND OBSTRUCTIVE LEFT HEART LESIONS

Although there are numerous mechanisms of LVOT obstruction, only valvar aortic stenosis and subaortic stenosis caused by discrete fibromuscular obstruction (subaortic membrane) or left ventricular hypertrophy are likely to be seen in unoperated adult patients. These will be discussed below. Multiplane TOE offers excellent imaging of the LVOT and rarely encountered causes of LVOT obstruction (for example supra aortic stenosis, accessory or anomalous mitral valve tissue, deviation or abnormality of the septum as part of complex congenital heart disease) should be identifiable by thorough examination.

From the mid oesophageal window, flexion at 0° produces a “five chamber” view in which the LVOT and base of the aortic valve leaflets are well visualised. Colour flow mapping in this view is useful for showing flow acceleration and turbulence at the site of obstruction. Rotating the image plane to 30° produces a short axis view at the base of the heart. Starting in an imaging plane below the aortic valve, gradual withdrawal of the probe produces transverse sections through the LVOT, the base, bodies and tips of the aortic valve leaflets, then the sinuses of Valsalva and coronary ostia. The plane is rotated to 130° where the subaortic region, aortic valve, and ascending aorta are examined in their long axis. Transgastric views of the LVOT, permitting satisfactory Doppler alignment (obtained by deep flexion at 0° or an oblique view between 110–140°) can be obtained in about 75% cases. Alternatively, the deep fundal view is used to obtain images analogous to TTE apical views.

Subaortic membrane

These may present in adults de novo or as a recurrence after previous resection. The membrane is a crescentic fibromuscular protuberance, attached medially to the ventricular septum just below the aortic valve, and laterally to the aorto-mitral junction or anterior mitral valve leaflet. The morphology of these lesions in adults may be complex, perhaps reflecting progression over time, and it is important to determine further attachments or involvement with the aortic valve leaflets. The subaortic membrane is most easily visualised in the long axis and five chamber views described above (fig 7). It is often difficult to image the crescentic nature and extent of the lesion in short axis. Subaortic membrane in adults is often accompanied by greater degree of left ventricular hypertrophy than expected. Upper septal

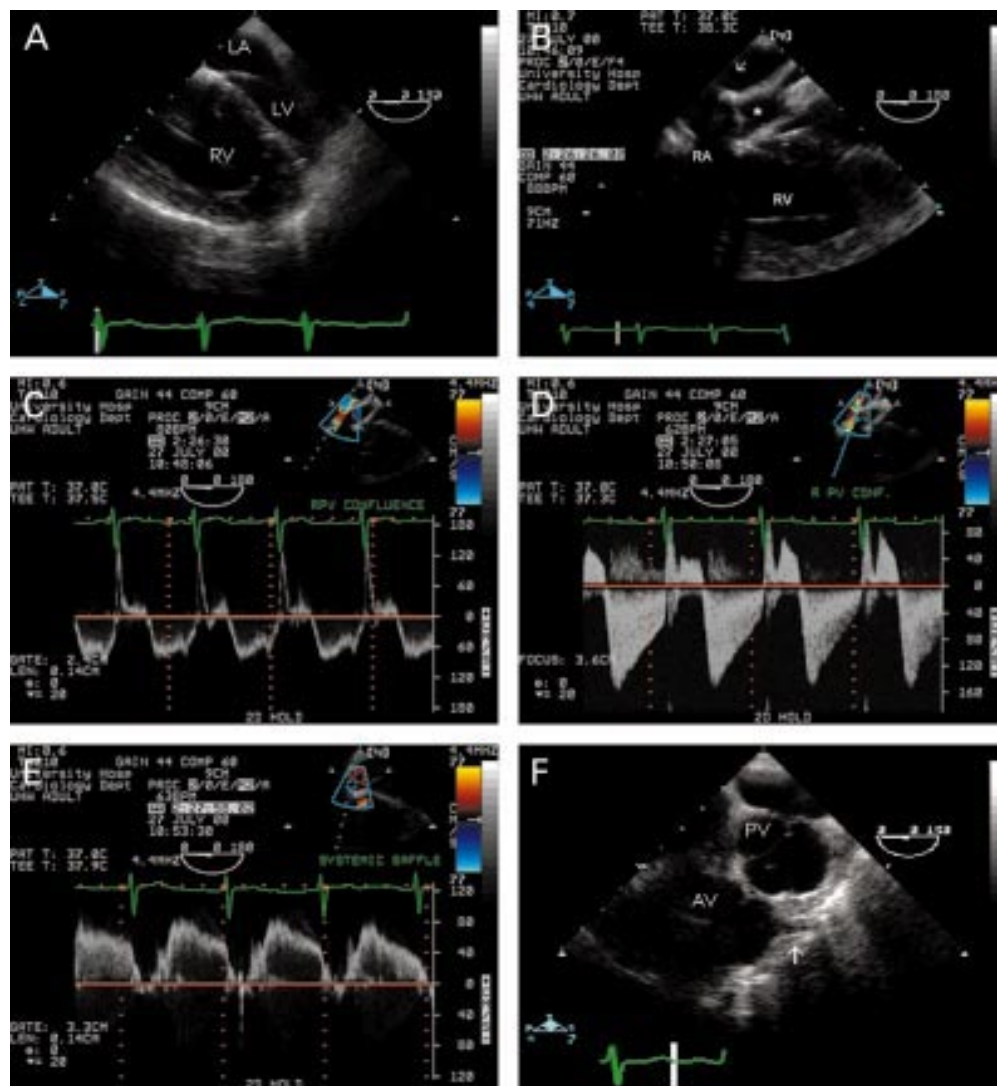


Figure 11 Transposition of the great arteries with Mustard procedure. The thick walled, dilated right ventricle and thin walled, compressed left ventricle (A) are typical of conditions in which the right ventricle is the systemic ventricle. The appearance of the posterior structures is complex (B). The pulmonary veins drain into a confluence (arrow) and then the right atrium. The systemic venous return is baffled (*) across to the left atrium. Colour and spectral Doppler interrogation of venous inflows must be scrupulous. Pulse wave Doppler at the pulmonary venous confluence shows a normal velocity and laminar (C) but, at the junction of the confluence and the right atrium there is turbulence, increased velocity indicating a small gradient (10 mm Hg), and an abnormal flow pattern (D). Flow within the systemic venous baffle was normal (E). Both great arteries are seen in parallel (F). The aorta is anterior and the origin of the left coronary artery well visualised. LA, left atrium; LV, left ventricle; RA, right atrium; PV, pulmonary valve; AV, aortic valve.

hypertrophy may contribute to LVOT obstruction. It is common for patients with subaortic stenosis to develop aortic regurgitation due to interference of leaflet closure by the membrane and/or premature degenerative disease. Thus, the aortic valve appearance, and the severity and mechanism of aortic regurgitation, must be studied carefully.

Congenital aortic valve disease

The valve leaflets may be thin and pliant or thickened, calcified, and restricted. In the short axis view, scanning at the leaflet tips reveals the number and arrangement of cusps—note that this is done with the leaflets open in systole (fig 8). Although unicuspid and quadricuspid valves have been reported in adults, the vast majority are bicuspid—either two symmetrical leaflets or fusion of two leaflets, with a midline raphe, often associated with asymmetric sinuses of Valsalva. In young patients in whom

there is little aortic valve calcification, transverse section scanning at the aortic valve leaflet tips (usually 30–60°) is used to obtain an accurate measure of aortic valve area. In the long axis, the hallmark sign of doming is best seen. In addition, “post-stenotic” dilatation (a misnomer) should be identified and measured (at aortic valve annulus, sinuses of Valsalva, sinotubular ridge, and ascending aorta). We use serial magnetic resonance imaging for accurate and reproducible follow up of aortic dilatation (and follow up of coarctation after surgery).

ASSESSMENT OF THE RIGHT VENTRICLE AND PULMONARY VALVE: OBSTRUCTIVE RIGHT HEART LESIONS

Pulmonary or subpulmonary stenosis may present or recur in adulthood, or develop as a consequence of RV hypertrophy from any cause. Severe right ventricular outflow tract



Figure 12 Complex congenital heart disease illustrating many of the points in the text. In the mid oesophageal 0° view (A), a single common atrium is seen. The atrioventricular valves are aligned and there is a large inlet ventricular septal defect (essentially producing a single ventricle) consistent with a common atrioventricular valve/complete atrioventricular septal defect. (B) Longitudinal image plane (120°). The aorta is seen anteriorly, connected to an anteriorly placed ventricle of indeterminate morphology. The pulmonary valve/artery cannot be seen. (C) Short axis view of the aortic valve and pulmonary valve (arrow). The ventriculo-arterial valves are arranged in a parallel fashion, with the aorta anterior, indicating malposed great arteries. The aortic valve orifice is triangular, suggesting a tricuspid valve. The pulmonary valve is small and the pulmonary artery was atretic in this case. The pulmonary valve orifice is oval, typical of a bicuspid (or unicuspid) valve. AV, aortic valve.

(RVOT) obstruction may be remarkably well tolerated. With recent advances in TTE imaging, the pulmonary valve can be often seen; haemodynamic assessment by colour flow mapping and spectral Doppler is usually sufficient to diagnose RVOT obstruction, pulmonary stenosis or regurgitation. Nevertheless, it is possible to obtain more detailed and better defined images of the right heart with TOE and, in patients with suboptimal TTE windows, TOE is very useful in determining the nature and severity of RVOT obstruction.

In the mid oesophageal four chamber view the RVOT cannot be seen, but the presence of RV hypertrophy and prominent trabeculations

forming a muscle band across the cavity may be seen. Rotation of the imaging plane to the short axis view (30°) separates RV inflow and outflow. The pulmonary valve leaflets may be difficult to see in patients with aortic root calcification. Further rotation to $90\text{--}130^\circ$, with the probe rotated to the right, reveals long axis views of the pulmonary valve and main pulmonary artery. Views of the pulmonary bifurcation are obtained in transverse (0°) scans in the upper oesophagus, from where the right pulmonary artery can be followed for several centimetres. The left pulmonary can rarely be seen beyond its origin. TOE is not an ideal technique for investigating branch pulmonary artery disease—angiography and magnetic resonance imaging are much better. The transgastric window affords excellent images of the RV. It is possible to align the Doppler signal to flow in the RVOT using a transgastric long axis view (fig 9), although this is a considerable distance from the probe tip and low transducer frequencies may be required.

Double chamber right ventricle

Mid cavity obstruction may develop secondary to any cause of RV hypertrophy—sometimes despite correction of the original problem such as a VSD (fig 9).

Subvalvar (infundibular) and valvar pulmonary stenosis

It is possible to differentiate subpulmonary stenosis—caused by abnormal hypertrophy of the infundibulum of the RV—from valvar pulmonary stenosis in the short axis and outflow views. Transverse views of the pulmonary valve are much more difficult to obtain than of the aortic valve and precise delineation of the leaflets may be impossible. However, doming of the leaflets is readily apparent (fig 10).

COMPLEX CONGENITAL HEART DISEASE: CORRECTIVE AND PALLIATIVE SURGERY

A detailed discussion of the follow up investigation of patients who have undergone corrective or palliative surgery for congenital heart disease is beyond the scope of this paper. Homografts and repaired tetralogy of Fallot are described briefly. TOE is valuable in the assessment of patients who have undergone “atrial switch” (Mustard or Senning) procedures for transposition of the great arteries, since the systemic venous baffle and pulmonary venous confluence are posterior structures. The echocardiographic approach has been described elsewhere²; the TOE appearance is illustrated and described briefly in fig 11. Complex congenital heart disease involving single ventricle systems (with or without a Fontan-type circuit) are not addressed here. An example of an adult patient with a single ventricle (and systemic-pulmonary arterial shunt) is shown in fig 12.

Homografts

Homografts are used in young patients undergoing a variety of corrective surgical procedures, typically RVOT repairs (Rastelli conduits, repair of tetralogy of Fallot) and aortic

root replacement. Over time, they are susceptible to calcific degeneration, causing homograft stenosis and/or regurgitation and endocarditis. These patients are often very difficult from the TTE approach, made worse by calcification of anterior structures. While TOE is better, detailed imaging is sometimes disappointing for the same reasons. The approach to scanning these patients is the same as described for RVOT and LVOT. In addition, attempts are made to image the upper and lower anastomoses of the grafts, where aneurysm, pseudoaneurysm or abscess formation can occur.

Repaired tetralogy of Fallot

Corrective surgery may involve resection of infundibular stenosis, pulmonary transannular patch, valveless or valved conduit, VSD closure and branch pulmonary artery dilatation. The long term sequelae of such radical repair are often right ventricular hypertrophy (RVH) and dilatation, pulmonary stenosis, and (severe) pulmonary regurgitation. In addition, there may be residual VSD leak. The aortic root is large and there may be aortic root dilatation.

Branch pulmonary stenosis is common but is poorly assessed by TOE.

Conclusions

TOE is a valuable and challenging technique in adult congenital heart disease. Combined expertise in echocardiography and congenital heart disease is required. A detailed standardised scanning protocol should be used and this approach is unfamiliar for many adult cardiologists. This is the very worst scenario in which to "stick the probe down and have a look".

- 1 Wren C, O'Sullivan JJ. Survival with congenital heart disease and need for follow up in adult life. *Heart* 2001;**85**:438-43.
- 2 Houston A, Hillis S, Lilley S, *et al.* Echocardiography in adult congenital heart disease. *Heart* 1998;**80**(suppl):S12-26.
- 3 Stumper O. Imaging the heart in adult congenital heart disease. *Heart* 1998;**80**:535-6.
- 4 Hirsch R, Kilner PJ, Connelly MS, *et al.* Diagnosis in adolescents and adults with congenital heart disease. Prospective assessment of individual and combined roles of magnetic resonance imaging and transesophageal echocardiography. *Circulation* 1994;**90**:2937-51.
- 5 Tynan MJ, Becker AE, Macartney FJ, *et al.* Nomenclature and classification of congenital heart disease. *Br Heart J* 1979;**41**:544-53.



Want to know more?

Data supplements

Limited space in printed journals means that interesting data and other material are often edited out of articles; however, limitless cyberspace means that we can include this information online. Look out for additional tables, references, illustrations, and (soon to appear) multimedia clips online!

www.heartjnl.com